Seismic behaviour of retaining structures: from fundamentals to performance-based design

Giulia M. B. Viggiani[1] and Riccardo Conti[2]

[1] University of Cambridge, Cambridge, UK
gv278@cam.ac.uk
[2] Università Niccolò Cusano, Rome, Italy
riccardo.conti@unicusano.it

Abstract. This lecture summarises research carried out by the Authors on the seismic behaviour of displacing or yielding retaining structures, *i.e.*, structures that can undergo permanent displacements during strong earthquakes without failing. For these systems, energy dissipation on shaking, leading to reduced inertia forces, can be achieved by allowing the activation of ductile plastic mechanisms. These must be correctly identified to guarantee the desired strength hierarchy, and depend on the specific retaining structure under examination. It will be shown that the critical acceleration, or the smallest value of acceleration corresponding to the activation of the critical plastic mechanism, is a key ingredient for performance based design of yielding retaining structures. In fact, the critical acceleration controls both the maximum internal forces on the structural elements and the magnitude and trend of post-seismic permanent settlements and rotations, required for quantitative serviceability and post-earthquake operability assessment of infrastructure. Based on a clear understanding of the physical mechanisms governing the dynamic behaviour of these systems, pseudostatic limit equilibrium solutions and simplified dynamic methods can be developed for their seismic design. Theoretical results are validated against data from reduced scale centrifuge models and the results of pseudo-static and fully dynamic numerical analyses. Finally, all the results presented in the paper, including experimental, numerical and theoretical findings, are used to provide suggestions for the performance-based design of retaining structures.

Keywords: Retaining Structures, Seismic Performance Based Design, Displacements.

1 Introduction

In contrast to other types of retaining structures, such as basement walls or bridge abutments, yielding walls are characterized by the absence of kinematic constraints preventing the occurrence of displacements in the retained soil, where active limit conditions can then develop, both under static and dynamic conditions. This class of retaining structures includes gravity and semi-gravity (cantilevered) walls, as well as embedded cantilevered, single-propped and anchored walls.

Field observations during recent earthquakes (Verdugo *et al.*, 2012; Wagner & Sitar, 2016) have shown that the overall performance of these structures is generally satisfactory and that the majority of damages affected either waterfront structures, due to the onset of liquefaction phenomena within the saturated backfill, or structures on slopes. However, even in these cases, it was recognised that, rather than catastrophic failures, many quay walls suffered from excessive displacements and deformations that compromised the serviceability of port facilities (Koseki *et al*., 2012).

Following the seminal works by Okabe (1926) and Mononobe & Matsuo (1929), the seismic design of earth-retaining structures is conventionally carried out using a force-based approach, in which dynamic actions are represented as pseudostatic forces proportional to an equivalent acceleration and the performance of the system is quantified conventionally in terms of a static safety factor against an assumed collapse mechanism (PIANC, 2001). In this framework, several studies have tackled the problem of computing pseudostatic earth pressures on retaining structures with theoretical (Lancellotta, 2007; Mylonakis *et al*., 2007), experimental (Atik & Sitar, 2010) or numerical methods (Evangelista *et al*., 2010). For yielding walls, the activation of plastic mechanisms within the soil-structure system makes the dynamic interaction problem a strength-driven rather than a deformability-driven problem. As a result, elastic solutions for the computation of the dynamic soil thrust (*e.g.*, Brandenberg *et al*., 2015) are of little applicability in this context.

The displacement-based approach, developed within the Performance-Based Design (PBD) methodology, provides a more rational approach to the seismic design of yielding structures. Following this approach, it is admitted that the soil-wall system can undergo permanent deformations under the design earthquake, provided that its overall behaviour is ductile and the residual displacements do not exceed admissible thresholds, prescribed based on the limit state under consideration. Broadly speaking, the rationale behind this approach is that in highly seismic areas it would be too expensive (if not impossible) to design a wall capable of withstanding the design earthquake without moving (Pender, 2019). Even when designing with the simpler force-based approach, the PBD methodology is implemented in modern codes (NTC, 2018; EC8, 2004) by linking the equivalent acceleration to be used in a pseudostatic calculation to the maximum displacement that the structure can sustain, with respect to different levels of the design earthquake.

In this context, the horizontal permanent displacement of the wall under a given design earthquake is usually taken as a performance indicator of the whole system (PIANC, 2001). Therefore, following the pioneering works by Newmark (1965) and Richards & Elms (1979), many works have been devoted to the computation of wall displacements (Ling, 2001; Huang *et al*., 2009; Conti *at al*., 2013; Cattoni *et al*., 2019; Callisto, 2019), most of them based on Newmark's rigid-block analysis.

Within this framework, the critical acceleration, a_c, corresponding to the full mobilisation of the strength of the system, turns out to be a key ingredient for both the geotechnical and structural design of the wall. In fact, a_c controls both the amount of permanent displacements of the wall at the end of the earthquake and the maximum internal forces that the structure may ever experience during an earthquake. In fact, the internal forces in the wall remain approximately constant for accelerations larger than

the critical acceleration, whereas no permanent displacements occur for accelerations lower than the critical value, at least for the case of sliding gravity and semi-gravity walls (Conti et al., 2013).

This lecture summarizes recent research on the dynamic behaviour of yielding retaining structures. Based on a clear understanding of the physical mechanisms governing the seismic response of these systems, pseudostatic limit equilibrium solutions and simplified dynamic methods were developed for their seismic design. Theoretical solutions were validated against data from reduced scale centrifuge models and the results of pseudostatic and fully dynamic numerical analyses. Finally, all the observations presented are used to provide suggestions for the performance based design of retaining structures.

The numerical analyses discussed in this work, for gravity, semi-gravity and embedded retaining structures were carried out in plane-strain conditions using the finite difference code FLAC v5 (Itasca, 2005). The soil was always modelled as an elastic-perfectly plastic material with a Mohr-Coulomb failure criterion and a non-associative flow rule, with zero dilatancy, combined with a hysteretic model making use of the Masing (1926) rules to describe the unloading-reloading behaviour under cyclic loading. Structural elements were modelled using elastic solid (gravity walls), beam (semi-gravity and embedded walls) and cable (tie-rods) elements. A pair of retaining walls facing each other were modelled in all dynamic analyses, in order to simplify the definition of lateral constraints. A horizontal acceleration time history was applied to the bottom nodes of the grid, while standard periodic constraints were applied to the lateral boundaries of the mesh. Both simple Ricker wavelets and real acceleration time histories were used as input, the latter covering a significant range of amplitudes and frequency contents.

2 Gravity and semi-gravity cantilever walls

In addition to sliding, field observations after the Kobe earthquake in 1995 revealed significant tilting of gravity and semi-gravity walls, clearly pointing at the activation of bearing capacity failure under dynamic loading (Anderson *et al*., 2008). Similar conclusions were drawn by Huang *et al*. (2009) and Conti *at al*. (2015), based on experimental data of shaking table and dynamic centrifuge tests on concrete gravity walls, respectively, and by Smith and Cubrinovski (2011) and Conti and Caputo (2019), based on the results of pseudostatic and dynamic numerical analyses.

In the light of Newmark's approach, translational (Ling, 2001; Conti *et al*., 2013) rotational (Zeng & Steedman, 2000) and bearing capacity (Huang, 2005) failure mechanisms have been considered in the literature to compute permanent displacements. However, only very recently attention was given to the relative importance of the three failure mechanisms in computing the critical acceleration of the wall (Kloukinas *et al*., 2015; Conti *et al*., 2015; Pender, 2019; Conti & Caputo, 2019). Centrifuge dynamic tests and numerical studies have shown that Newmark's rigid-block analysis provides good results when applied to gravity retaining structures, either sliding or rotating on their base (Zeng & Steedman, 2000; Conti *et al*., 2013). On the other hand, predictions

turn out to be less satisfactory in the case of combined sliding and rotating plastic mechanism, induced by a bearing capacity failure of the foundation soil (Conti and Caputo, 2019).

Regarding the seismic behaviour of cantilevered walls, two further issues are the applicability of the Mononobe-Okabe (MO) theory in computing the dynamic soil thrust and the possible phase shift between the maximum value of the soil thrust and the inertia forces into the wall-soil system. Both issues affect the computation of maximum structural internal forces and result in quite controversial recommendations for the structural design of these structures under seismic conditions (AASHTO, 2012).

2.1 Plastic mechanisms and critical acceleration

For the sake of simplicity, theoretical computation of the critical acceleration and of the earthquake-induced permanent displacements are typically carried out neglecting both the vertical input acceleration, $a_v(t)$, and any possible change in the system geometry during the applied earthquake. Indeed, assuming a pure horizontal input acceleration ($k_v = 0$) and a fixed geometry of the soil-wall system, the yield acceleration of the wall, related to the activation of a given plastic mechanism, $a_y = k_y g$, is a property of the sole system and does not depend on the applied input acceleration.

Regarding the first assumption, $a_v(t)$ is generally out of phase with and has a different frequency content than the horizontal acceleration, $a_h(t)$, with the corresponding peak values never occurring simultaneously. Therefore, positive and negative contributions from $a_v(t)$, on average, have little effect on the dynamic response of retaining structures and can be reasonably overlooked without significant loss of accuracy (Garini *et al*., 2011). In relation to the second assumption, changes in the system geometry during shaking have no relevant effects on the computation of the final permanent displacement, at least for ratios of the critical acceleration of the wall and the maximum horizontal input acceleration, $a_c/a_{max} \geq 0.2$, *i.e.*, for well-designed walls (Stamatopoulos *et al*., 2006). Conti *et al*. (2013) came to a similar conclusion, showing that the failing soil wedge remains approximately constant during sliding, and the same as at the onset of sliding.

To provide a consistent theoretical framework for the computation of the critical acceleration of gravity and cantilever walls, Conti and Caputo (2019) and Pender (2019), showed that these structures accumulate permanent displacements either by sliding on their base or by bearing capacity failure of the foundation soil. As a result, a_c can be computed as:

$$a_c = \min\left(a_{y,SLID}, a_{y,QLIM}\right) \tag{1}$$

where $a_{y,SLID}$ and $a_{y,QLIM}$ are the pseudostatic yield accelerations corresponding to which the strength of the system is fully mobilised under a pure sliding mechanism (Richards & Elms, 1979) and a bearing capacity failure (Conti, 2018), respectively.

The type of plastic mechanism effectively mobilised within the soil-wall system depends ultimately on the strength properties of the backfill and the foundation soil. In the case of walls resting on cohesionless soils, experimental data (Conti *et al*., 2015; Kloukinas *et al*., 2015; Koseki *et al*., 2003), numerical results (Smith & Cubrinovski,

2011; Conti & Caputo, 2019) and theoretical studies (Pender, 2019) have shown that the bearing capacity failure is likely to be the 'natural' failure mechanism. More in general, Figure 1 shows the results of a parametric study carried out by Viggiani and Conti (2016), highlighting the role played by the cohesion of the foundation soil on the critical failure mechanism of gravity walls. Also, numerical and theoretical results for cantilever walls on fine-grained soils indicate that the sliding mechanism usually controls the dynamic behaviour of the wall in undrained conditions (Conti & Caputo, 2019).

A powerful tool for investigating the behaviour of the soil-wall system under critical (limit equilibrium) conditions is provided by numerical pseudostatic analyses, which permit to investigate both the shape of the plastic mechanism induced by a uniform horizontal acceleration field and the value of the critical pseudostatic coefficient, $k_c = a_c/g$, corresponding to which the mechanism is activated.

Conti and Caputo (2019) conducted an extensive numerical parametric study on semi-gravity cantilever walls, highlighting the behaviour of such systems under both pseudostatic and dynamic (earthquake) excitations. The Authors considered three different geometries for the wall and two different soil deposits, including a cohesionless and a cohesive soil layer immediately beneath the foundation, with drained (D) and undrained (UD) behaviour respectively.

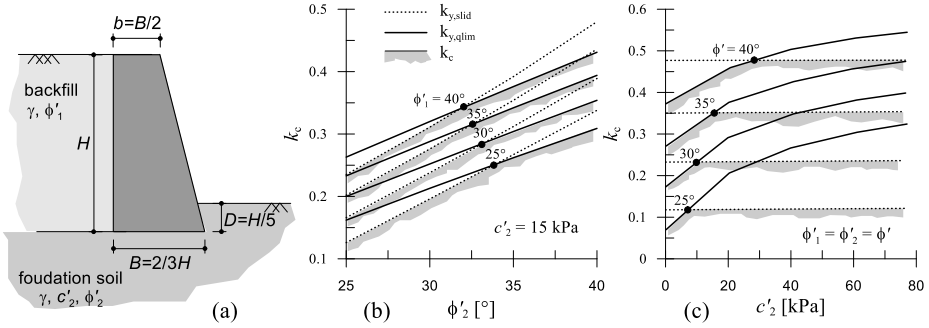

Fig. 1. Gravity walls: (a) wall layout; (b) dependence of k_c on ϕ'_1 and ϕ'_2, for c'_2 = 15 kPa; (c) dependence of kc on c'_2, for $\phi'_1 = \phi'_2 = \phi'$.

Figure 2 shows one of the layouts considered in their work (W2), designed to have a proper static safety factor under drained (D) and undrained (UD) conditions. For this layout, Figure 3 shows the contours of shear strains computed in pseudostatic critical conditions, together with the critical failure mechanism predicted by theoretical methods. In drained conditions (Fig. 3a) the plastic mechanism involves the development of shear deformations within the supporting soil, related to the bearing failure of the foundation, eventually leading to both sliding and rotation of the wall. On the other hand, in undrained conditions (Fig. 3b), the critical mechanism corresponds essentially to pure sliding of the wall along its base. Numerical and theoretical results show some discrepancies in terms of the shape of the slip surfaces, but the predicted values of k_c are in very good agreement, both in drained and undrained conditions.

The results indicate that the critical acceleration controls the dynamic behaviour of semi-gravity walls under real earthquake inputs. Figure 4 shows the maximum acceleration computed at mid height of the vertical stem ($a_{max.MID}$) against the maximum free-field acceleration ($a_{max.ff}$), for the drained (a) and the undrained (b) analyses, together with the theoretical values of the critical acceleration. Maximum rightwards ($a_{max.MID}$, $a_{max.ff}$) and leftwards ($|a_{min.MID}|$, $|a_{min,ff}|$) accelerations are considered for the right and the left wall respectively. As expected, once the critical threshold is attained (*i.e.*, as soon as a plastic mechanism develops in the soil-wall system), the absolute acceleration of the system remains approximately constant, starting to deviate from the free-field excitation. Theoretical predictions of a_c are in good agreement with the numerical dynamic results.

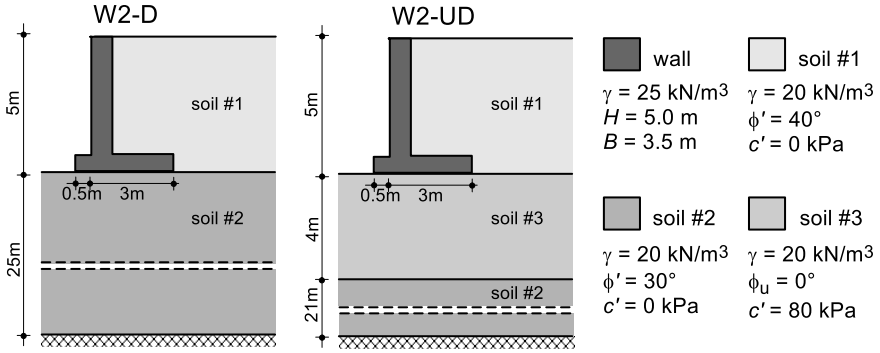

Fig. 2. Semi-gravity cantilever walls: layout analysed in pseudostatic and dynamic numerical analyses (modified after Conti & Caputo, 2019).

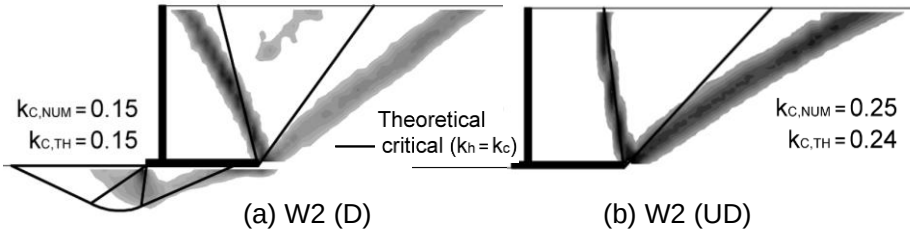

Fig. 3. Pseudostatic numerical analyses of semi-gravity cantilever walls: contours of shear strains at the onset of critical conditions and comparison with theoretical predictions: layout W2 in drained (a) and undrained (b) conditions (modified after Conti & Caputo, 2019).

2.2 Structural internal forces

Figure 5(a) shows the forces acting on the soil-wall system under the horizontal ($a_h = k_h g$) and vertical ($a_v = k_v g$) pseudostatic accelerations, even if the latter are usually neglected. Both the dynamic active soil thrust acting on the vertical plane AV, S_{AE}, its inclination on the horizontal, δ_S, and the inclination of the two failure surfaces, ω_α and ω_β, were derived by Kloukinas & Mylonakis (2011) by rigorous plasticity solutions.

When dealing with the internal stability of the vertical stem (structural design), the soil thrust effectively acting on its back (S_E) must be taken into account, resulting from the dynamic interaction between the soil volume above the heel and the wall (Fig. 5(b)). Table 1 reports two possible approximate solutions for $S_{E,h}$. In the first case (S1), it is assumed that no shear stresses develop at the contact between the heel and the soil above it ($T_E = 0$), and hence the soil thrust S_{AE} and the inertia forces $k_h W_s$ are entirely transferred to the vertical stem. The second solution (S2) assumes that the soil volume above the heel is in active limit state conditions and that the presence of the horizontal stem does not alter the resulting soil thrust. In this condition, S_E can be computed using the Mononobe-Okabe (MO) theory.

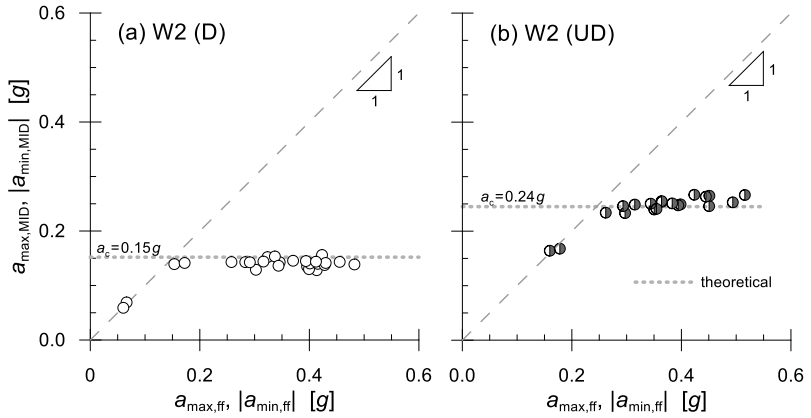

Fig. 4. Dynamic numerical analyses of cantilever walls: Maximum wall horizontal acceleration as a function of the maximum free-field acceleration, for layouts: (a) W2 (D) and (b) W2 (UD) (modified after Conti and Caputo, 2019).

Figure 6 shows, for layouts W2-D and W2-UD, the maximum normalised bending moment computed under the applied earthquakes, $M_{max}/\gamma H^3$, as a function of the maximum free-field acceleration (Conti & Caputo, 2019). The approximate solutions S1(k_h), S1(k_c) and S2(k_h) are also plotted for comparison. The maximum bending moment can increase even for $a_{max,ff} > a_c$, even though the absolute acceleration of the system remains constant (see *e.g.*, Fig. 4), due to an internal redistribution of stresses leading to a reduction of T_E. Nonetheless, the solution S1(k_c), corresponding to $T_E = 0$, always defines the upper bound for M_{max}. Moreover, as long as this limiting condition is not achieved, the solution S2($k_h = a_{max,ff}/g$) provides a reasonable estimate of the maximum internal forces in the stem, with a maximum relative scatter of about 20% with respect to the numerical values.

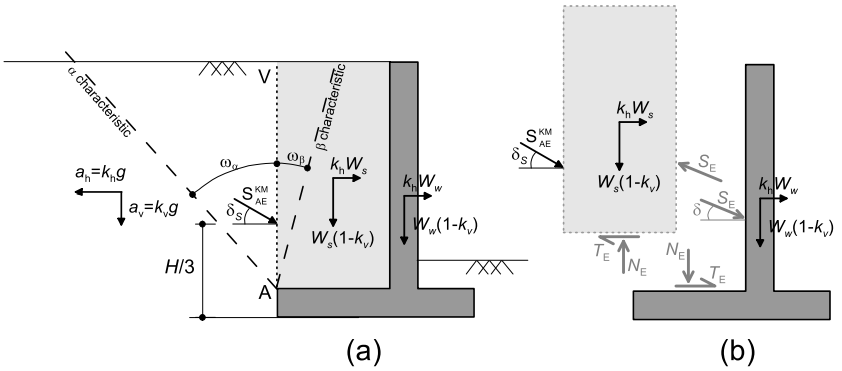

Fig. 5. Semi-gravity cantilever walls: (a) system of pseudostatic external forces; (b) assessment of the internal stability (modified after Conti & Caputo, 2019).

Table 1. Semi-gravity cantilever walls: approximate theoretical solutions for the horizontal force acting on the vertical stem.

Solution	$S_{E,h}$	M_{max}
$S1(k_h)$	$S^{KM}_{AE,h}(k_h) + k_hW_s$	$S^{KM}_{AE,h}(k_h)\cdot H/3 + k_h(W_{w,stem}+W_s)\cdot H/2$
$S2(k_h)$	$S^{MO}_{AE,h}(k_h)$	$S^{MO}_{AE,h}(k_h)\cdot H/3 + k_hW_{w,stem}\cdot H/2$

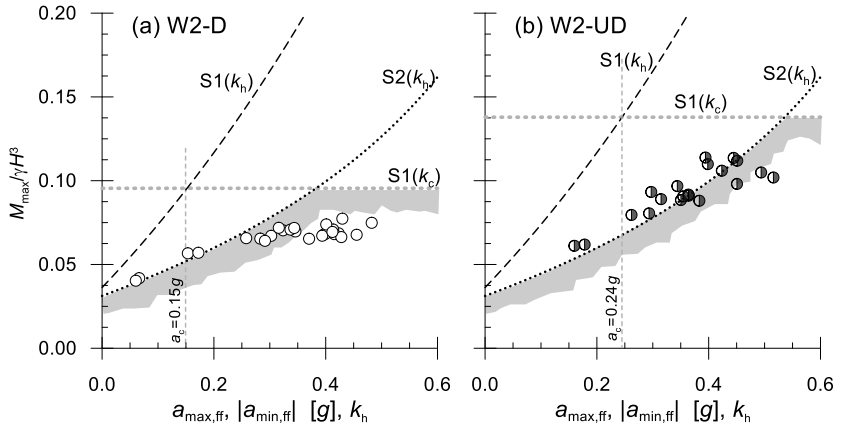

Fig. 6. Dynamic numerical analyses of semi-gravity cantilever walls: Maximum bending moment on the vertical stem as a function of the maximum free-field acceleration, for layouts: (a) W2 (D) and (b) W2 (UD) (modified after Conti and Caputo, 2019).

Based on numerical results, Conti and Caputo (2019) drew the following conclusions regarding the forces acting on the wall and the accelerations in the soil-wall system:

- During a dynamic event, the maximum values of $S_{E,h}$ and of the structural bending moment are always in phase and occur when the inertia forces into the system are directed away from the backfill.

- Possible phase shifts can occur between free field and wall accelerations, when the wall undergoes permanent displacements. Moreover, the actual average acceleration of the soil-wall system can differ significantly from the free-field one, its physical upper bound corresponding to the critical value a_c.
- Up to the critical condition ($k_h \leq k_c$, where $k_h = a_{max,ff}/g$), MO pseudostatic solution provides a good estimate of the active soil thrust acting on the vertical stem.
- As soon as a plastic mechanism develops within the soil-wall system ($k_h > k_c$), the average absolute acceleration of the system remains constant. Therefore, also the maximum inertia force that the system can ever experience during an earthquake is bounded by its critical value. Moreover, the pseudostatic solution S1(k_c) (corresponding to $T_E = 0$) defines the upper bound for $S_{Eh,max}$ and M_{max}.
- The maximum internal forces in the wall ($S_{Eh,max}$, M_{max}) can increase even for $k_h > k_c$, even though the absolute acceleration of the system remains constant, due to an internal redistribution of stresses leading to a reduction of T_E. This behaviour cannot be predicted within a perfect plasticity framework, as it depends on the amounts of shear deformations at the contact between the heel and the soil above it. However, from a practical point of view, the solution S2(k_h) provides a reasonable estimate of the structural internal forces until the limiting condition S1(k_c) is achieved.

2.3 Displacements

The plastic mechanism activated within the soil-wall system governs both the value of the critical acceleration and the pattern of permanent displacements that the wall may undergo during an applied earthquake. Any theoretical model for the computation of permanent wall displacements must take into account properly the kinematics effectively activated within the soil-wall system once the critical acceleration is exceeded.

Conti *et al*. (2013) proposed a Newmark's like theoretical model for the computation of permanent displacements of gravity and semi-gravity walls sliding on a rigid base. Exploiting the analogy between the wall-soil wedge system and an elementary system comprising two-rigid blocks sliding on an inclined plane, the Authors showed that the dynamic equilibrium of the system can be written as:

$$-\ddot{u}_r(t) = \eta \cdot [k_h(t) - k_c]g \tag{2}$$

where $\ddot{u}_r$ is the horizontal relative acceleration of the wall, $k_h(t) = a_h(t)/g$ is the base horizontal acceleration and $k_c = a_c/g$ is the critical acceleration corresponding to a sliding mechanism, which can be computed as:

$$k_c = \frac{W_w \tan\phi_b - S_{AE}[\cos(\delta+\beta) - \sin(\delta+\beta)\tan\phi_b]}{W_w} \tag{3}$$

Eq. (3) corresponds with the implicit equation proposed by Richards and Elms (1979). Coefficient η in Eq. (2) depends solely on the mechanical and geometrical properties of the system, and can be computed as:

$$\eta = \frac{\cos\phi_b \cos(\delta+\beta+\phi-\alpha) + (W/W_w)\cos(\phi-\alpha)\cos(\delta+\beta+\phi_b)}{\cos\phi_b \cos(\delta+\beta+\phi-\alpha) + (W/W_w)\cdot\frac{\cos\phi\cos\beta\cos(\delta+\beta+\phi_b)}{\cos(\alpha-\beta)}} \tag{4}$$

where the quantities α, β, δ and W_w are defined in Figure 7 for gravity (a) and semi-gravity (b) walls, respectively.

The ability of the proposed model to describe the dynamic behaviour of gravity walls was tested against the results of two plane-strain finite difference analyses of a pair of gravity walls retaining a 4 m thick ideal layer of dry sand overlying a stiffer soft rock deposit (Conti *et al*., 2013). The acceleration time history is a simple wavelet with a maximum acceleration of 0.3g in the first analysis, while it corresponds to a real rock outcrop earthquake recording in the second case (Tolmezzo earthquake: a_{max} = 0.35g, mean period T_m = 0.4 s, duration $T_{5\text{-}95}$ = 4.2 s).

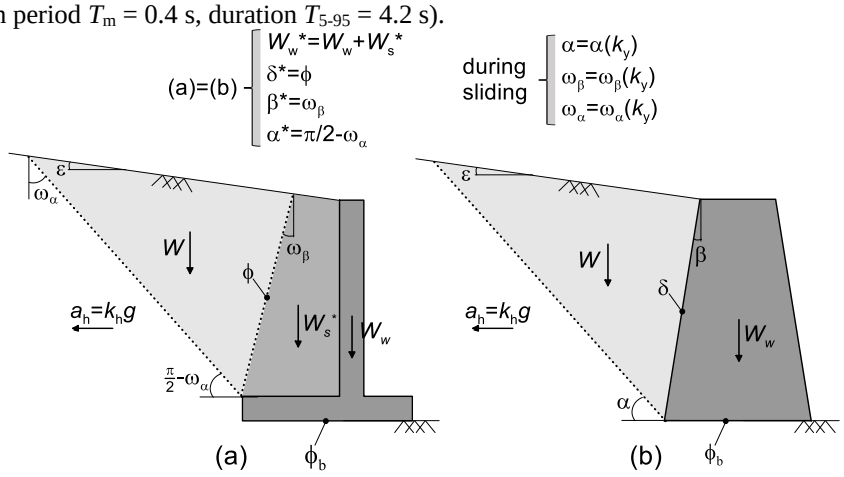

Fig. 7. Double wedge model for (a) cantilever and (b) gravity retaining walls, sliding along their base.

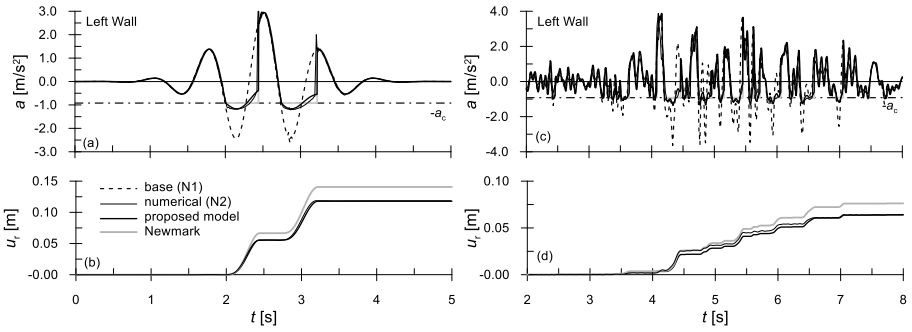

Fig. 8. Gravity walls: Comparison of numerical and model predictions: (a) absolute horizontal acceleration and (b) relative displacements of the left wall. Wavelet (left) and Tolmezzo (right).

According to the model described above, it is: k_c = 0.09 and η = 0.83. Figure 8 shows the results obtained from the numerical analyses in terms of computed absolute acceleration and relative displacements of the left wall. These are compared with the predictions obtained with the model described above, using the free field acceleration as the input base motion. The results show that the absolute acceleration of the wall coincides

with the base acceleration until the seismic coefficient is smaller than the critical value. Once the base acceleration exceeds k_c, the wall slides on its base under an absolute acceleration that varies with time, both in the numerical and theoretical models, while in the standard Newmark's approach ($\eta = 1$) the absolute acceleration of the wall during sliding is taken to be constant and equal to its critical value. The agreement between numerical and theoretical predictions is extremely good, both in magnitude and trend; on the other hand, a prediction obtained by direct application of Newmark's method over predicts the numerical displacement by about 17%.

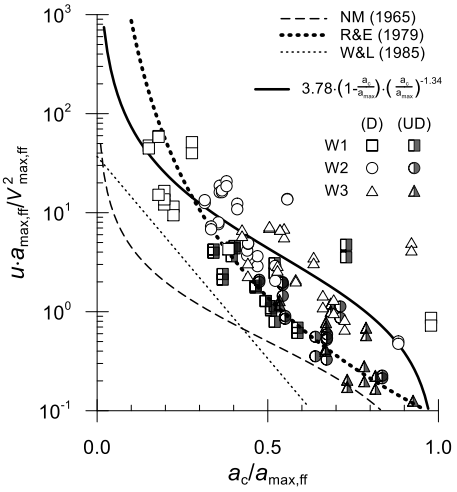

Fig. 9. Semi-gravity walls. Results of numerical dynamic analyses (Conti ad Caputo, 2019): normalised final horizontal displacement of the top of the wall as a function of $a_c/a_{max,ff}$.

Newmark's like methods based on the sliding block assumption do not provide reliable predictions when the plastic mechanism comprises both translation and rotation of the wall, as in the case of a bearing failure of the foundation soil. This fact is evident by inspection of Figure 9, collecting all the numerical results obtained by Conti and Caputo (2019) for cantilever wall layouts subjected to real earthquakes. Specifically, Figure 9 shows the final normalised displacement of the top of the wall, $u \cdot a_{max,ff}/V^2_{max,ff}$, where $V_{max,ff}$ is the maximum velocity computed in free-field conditions, as a function of the ratio $a_c/a_{max,ff}$ between the critical acceleration and the maximum free-field acceleration. Figure 9 also reports some of the interpolating functions proposed in the literature, all derived from the application of the Newmark's sliding block procedure (Newmark, 1965; Richards & Elms, 1979; Whitman & Liao, 1985), together with the best fit of the numerical results. Full and open symbols refer to the undrained (UD) and drained (D) foundation soil, where the activated plastic mechanism is pure sliding and bearing failure, respectively. As expected, the computed displacements reduce with increasing $a_c/a_{max,ff}$. However, while the numerical results for the undrained (UD) foundation soil are in satisfactory agreement with the equation proposed by Richards & Elms (1979) for sliding walls, those corresponding to the drained (D) profile are always above the

empirical relationships. This observation suggests that the available equations, all derived from the analysis of a rigid block sliding over a horizontal plane, can lead to non-conservative results if applied to retaining walls for which the permanent displacement stems from a combination of both sliding and rotation.

2.4 Suggestions for design

As far as the geotechnical design is concerned, the concept of an admissible wall displacement has been widely accepted within the PBD philosophy. However, the possibility of admitting wall tilting, related to a temporary attainment of the bearing resistance, is still a controversial issue. Indeed, many provisions and codes of practice still recommend to design the wall ensuring an adequate safety margin with respect to a bearing failure of the foundation and assuming the sliding mechanism as the critical one. The rationale behind it is twofold: (1) excessive wall tilting could induce brittle collapse of the wall by overturning; (2) no reliable procedures are available to accommodate a mixed sliding-rotational failure mode within the well-established Newmark's approach (Pender *et al*., 2019).

With this respect, a rational seismic design of gravity and semi-gravity walls should contemplate the possible activation of both mechanisms, instead of excluding a priori the expected rotation. In fact, the temporary mobilization of the soil shear strength beneath the foundation would not lead to a fragile failure of the system, provided that tilting of the wall is not excessive. This is a fundamental difference with respect to a pure overturning mechanism, which is indeed an intrinsically brittle mechanism. On the other hand, further research is required to develop reliable (and simple) theoretical models, capable of handling combined tilting and sliding failure modes as, in this case, a direct application of the Newmark's sliding block procedure can lead to significant under-prediction of the final displacement (Conti & Caputo, 2019).

Moving to the structural design of cantilever retaining walls, a simple three-step procedure can be defined to take into account, though approximately, the possible contribution of the horizontal stem to the overall dynamic equilibrium, as observed in numerical dynamic analyses (Conti & Caputo, 2019):

1. compute the critical acceleration of the wall;
2. use S1(k_c) to compute the maximum internal forces that the wall could ever experience during an earthquake;
3. for a given design earthquake, corresponding to which $k_h = a_{max,ff}/g$, use the min[S2(k_h), S1(k_c)] to compute the internal forces in the wall.

3 Embedded cantilevered and anchored walls

A number of factors make the seismic behaviour of yielding embedded retaining structures different from what observed in the case of gravity and semi-gravity walls, also affecting their seismic design:

- Both numerical analyses (Conti *et al*., 2014; Caputo *et al*., 2019) and experimental results (Conti *et al*., 2012; Fusco *et al*., 2019; Fusco, 2022), indicate that the stability of embedded retaining walls is guaranteed by the soil passive strength below dredge level. This always requires some permanent displacement in order to be fully mobilised, thus making the rigid perfectly plastic assumption not conservative in most cases.
- The definition of the critical plastic mechanism is not trivial, given that no simple equivalent "sliding block" can be identified, particularly when different failure mechanisms can be recognised for the soil-wall system, each one characterised by its own value of the yielding acceleration (Caputo *et al*., 2021).
- The collapse mechanism is often characterised by diffuse plastic deformations, and the associated displacement field cannot be reduced to a simple translational or rotational rigid body motion (Oliynyk *et al*., 2022).
- The soil volume interacting with the wall can be composed of layers of different mechanical properties and phase-shift of accelerations can occur along the height of the wall during the earthquake. In the majority of cases, however, both aspects are of less relevance for cantilevered and single-restrained embedded walls, with typical heights in the range of 10-20 m.
- Computation of internal forces is always a fundamental task for the structural design of these structures, requiring simple and reliable methods for the evaluation of pseudostatic contact earth-pressure distributions. These methods provide also the theoretical basis for the assessment of the critical acceleration for the soil-wall system.

The following sections will present the limit equilibrium methods proposed by Conti and Viggiani (2013) and Caputo *et al*. (2021) for the analysis of embedded cantilevered and anchored walls, inspired by the behaviour observed in numerical pseudostatic and dynamic simulations, overcoming limitations of standard approaches available in the literature. The attention will be placed on Steel Sheet Pile walls with shallow passive Anchors (ASSP) in the form of continuous sheet piles, rather than grouted anchors and propped walls, even if they show essentially the same dynamic behaviour of ASSP walls. The reader can refer to Conti *et al*. (2012) and Callisto and Dal Brocco (2015) for a thorough discussion on these structures.

Final considerations on the permanent displacements accumulated by these structures during earthquakes, and on available theoretical methods for their estimation, will be also provided.

3.1 Embedded cantilevered walls

Numerical dynamic analyses carried out by Conti *et al*. (2014) and Conti (2017) led to the following main conclusions:

- the passive resistance of the soil in front of the wall is mobilised progressively during the earthquake, starting from dredge level downwards: the stronger the applied acceleration, the greater the depth down to which the passive resistance is fully mobilised;

- in the time instants when the internal forces in the wall attain their maximum, the accelerations in the soil below dredge level are only a small fraction of the maximum value computed on the retained side, and always lower than about 0.1*g*;
- permanent displacements of the wall correspond to an approximately rigid rotation around a pivot point located at a depth of between 0.8×*d* and 0.9×*d*, where *d* is the embedment depth.

Figure 10 shows the horizontal earth pressure distribution assumed in the limit equilibrium method proposed by Conti and Viggiani (2013). For a given $k_h < k_c$ (continuous line), the soil on the retained side is in active limit state down to d_0, and in passive limit state below the rotation point. On the excavated side, the passive resistance of the soil is fully mobilised down to a depth $\bar{d}$; the soil is in active limit state below the pivot point, and the horizontal contact stress decrease linearly with depth between $\bar{d}$ and d_0. Moreover, it is assumed that the passive earth pressure coefficient takes its static value, K_P.

In critical conditions ($k_h = k_c$) the passive resistance of the soil below the excavation is mobilised completely down to the pivot point, i.e. $\bar{d} = d_0$, with d_0 about 0.9×*d* (dashed line in Fig. 10).

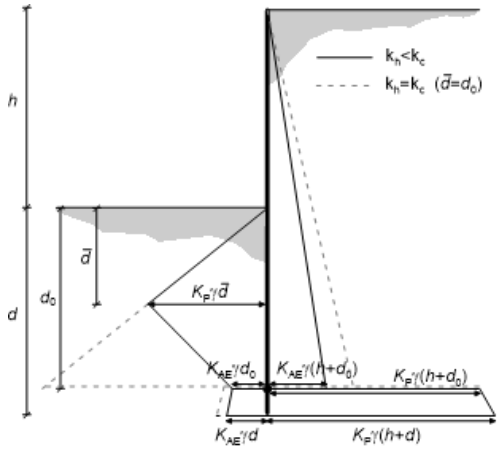

Fig. 10. Embedded cantilevered wall: theoretical pseudostatic earth pressure distribution (from Conti & Viggiani, 2013).

A comparison between numerical results and limit equilibrium calculations is shown in Figure 11, where the normalised maximum bending moments on the walls are plotted against the maximum accelerations computed behind the walls during the earthquakes (Conti *et al*., 2014). The proposed method is in good agreement with the numerical data and always provides conservative values of the maximum (critical) bending moment. The results show that for increasing strength of the soil-wall system, that is for increasing values of the soil and soil-wall friction angle and for increasing embedded depth, both the critical acceleration and the maximum bending moment increase. In other

words, a stronger soil-wall system will experience smaller displacements during the earthquake, but this is paid for by increasing internal forces in the wall.

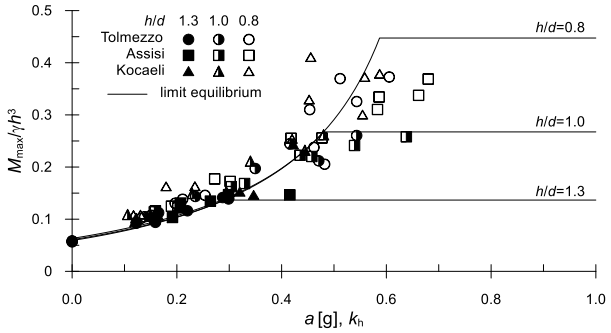

Fig. 11. Embedded cantilevered wall: maximum normalised bending moments computed from dynamic numerical simulations and limit equilibrium ($\phi' = 35°$, $\delta = 20°$, $\gamma = 20$ kN/m^3, $h = 4$ m) (from Conti & Viggiani, 2013).

3.2 Anchored Steel Sheet Pile (ASSP) walls

In the case of ASSP walls, the potential plastic mechanisms to examine involve a full mobilization of the shear strength in the soil, as their seismic design does not rely (typically) upon the ductility of the structural members. Specifically, three failure mechanisms can be identified: (1) attainment of the anchor capacity (anchor failure, $a_{y,AF}$); (2) complete mobilisation of the soil passive strength below dredge level (toe failure, $a_{y,TF}$); and (3) activation of a global mechanism, involving the wall, the anchor plate and the soil volume interacting with them (global failure, $a_{y,GF}$). Once the accelerations corresponding to each mechanism are computed, then the critical acceleration is given by:

$$a_c = \min\left(a_{y,AF}, a_{y,TF}, a_{y,GF}\right) \tag{5}$$

The possible occurrence of different plastic mechanisms was confirmed by numerical analyses (Caputo *et al*., 2021) and experimental results from dynamic centrifuge tests on reduced scale models of ASSP walls embedded in dry sand (Fusco *et al*., 2019). As an example, Figures 12(a) and (b) report the contours of vertical displacements measured at the end two earthquakes applied in Tests AF03 and AF04, whose layouts, according to limit equilibrium calculations, should correspond to anchor failure and global failure, respectively. Indeed, in Test AF03, the soil horizontal displacements occurred mostly in front of the anchor and in a wedge behind the main wall, showing the typical features of a local anchor failure. In contrast, during Test AF04, the soil included between the anchor, the main wall, and a curved surface extending between the two, experienced a nearly uniform horizontal displacement, confirming the predicted global failure.

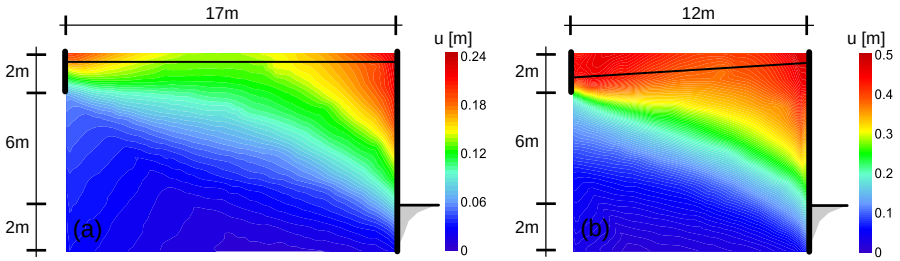

Fig. 12. ASSP walls: contours of horizontal displacements measured in two dynamic centrifuge tests (Fusco *et al*., 2021): (a) Test AF03, at the end of earthquake EQ3; (b) Test AF04, at the end of earthquake EQ2.

Figure 13 shows the theoretical earth pressure distributions assumed in the pseudostatic limit equilibrium method developed by Caputo *et al*. (2021) to assess (a) the maximum internal forces in the structural members and (b) the anchor capacity, T_{lim}. The former is consistent with a quasi-rigid rotation of the wall around a pivot point in the embedded portion. Specifically, for a given k_h, the soil is in active (retained side) and passive (below dredge level) limit condition down to a depth D^*. At larger depths, contact pressures are no longer related to a limit state condition and a simplified linear distribution is assumed.

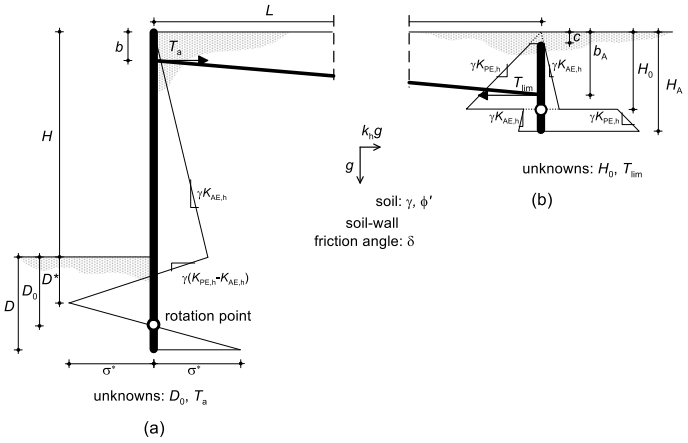

Fig. 13. ASSP walls: typical layout and theoretical pseudostatic earth pressure distribution (from Caputo *et al*., 2021).

The predicted capabilities of the new limit equilibrium method were assessed against the results of pseudostatic and dynamic numerical analyses. Figure 14 shows the normalized maximum bending moment, $M_{max}/\gamma H^3$, and axial force, $T_a/\gamma H^2$, as a function of k_h, for one of the layouts analysed by the Authors (H = 10 m; b_A/H_A = 1/3; L/H = 2.1; D/H = 0.4; ϕ' = 35°; γ = 20 kN/m^3). For $k_h < k_c$, LE predictions slightly overestimate the bending moment and underestimate the anchor force, while the method predicts

correctly the critical values. Once again, maximum internal forces are basically independent of the earthquake intensity and turn out to be a property of the system.

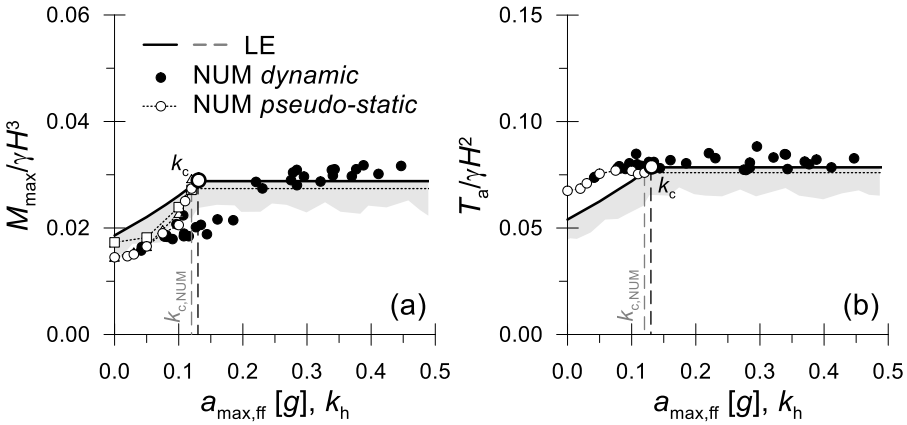

Fig. 14. ASSP walls: Comparison between numerical pseudostatic and dynamic analyses and LE predictions in terms of (a) $M_{max}/\gamma H^3$ and (b) $T_a/\gamma H^2$ (modified after Caputo *et al*., 2021).

3.3 Displacements of embedded retaining structures

Figure 15 shows the numerical values of the final permanent displacement computed at the top of embedded cantilevered (a) and ASSP (b) walls subjected to real earthquakes, as a function of $a_c/a_{max,ff}$ (Conti *et al*., 2014; Caputo *et al*., 2019). Contrary to what observed for gravity and semi-gravity walls, significant displacements occur for $a_c/a_{max,ff} > 1$, that is before the strength of the system is fully mobilized. This is consistent with the experimental observations by Conti *et al.* (2012), indicating that embedded walls may accumulate rigid permanent displacements concurrently with an increase of the internal forces in the structural members, that is before attaining the critical acceleration. This behaviour is due to a stress redistribution and a progressive mobilisation of the soil strength on the passive side of the wall produced by the earthquake (Conti *et al*., 2014; Conti, 2017).

The results shown in Figure 15 have two relevant implications for design. Firstly, allowable displacements less than about 0.1-0.2 m would result in a ratio $a_c/a_{max,ff} > 1$: that is, the wall should be designed to have a critical acceleration larger than the maximum acceleration expected at the site (*i.e.*, using an equivalent acceleration that is larger than the maximum free-field acceleration). This is completely different from the performance-based design of gravity retaining walls, as they will experience permanent displacements only if $a_c/a_{max,ff} < 1$. Secondly, application of Newmark's like procedures, based on the rigid perfectly-plastic soil assumption, would yield displacements that are much smaller than observed, as the analysis would overlook the displacements experienced by the wall before the acceleration reaches its critical value.

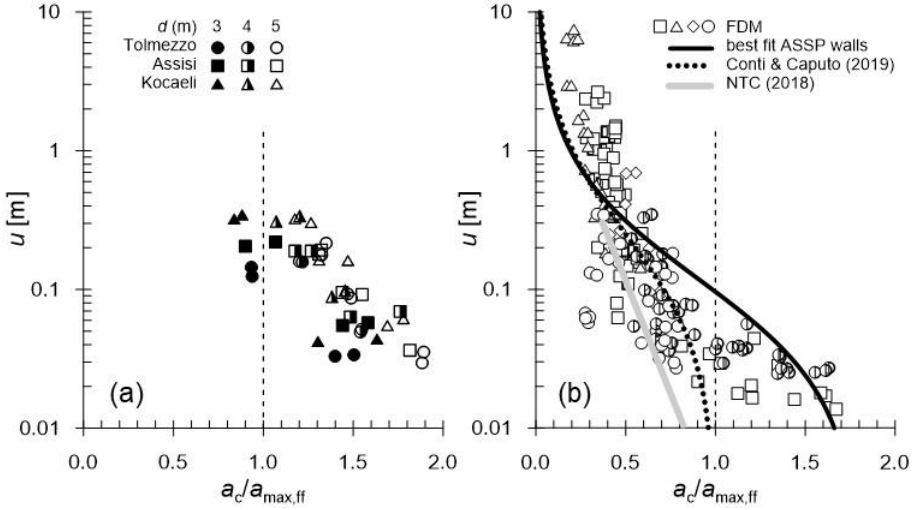

Fig. 15. Results of numerical dynamic analyses for (a) Embedded Cantilevered and (b) ASSP walls: final horizontal displacement of the top of the wall as a function of the ratio $a_c/a_{max,ff}$

4 Conclusions

Research carried out by the authors on the seismic behaviour of displacing or yielding retaining structures shows that the key ingredient for their performance-based design is the critical acceleration, controlling both the maximum internal forces that a retaining structure may experience during the earthquake and its permanent displacements at the end of the earthquake.

The critical acceleration may be defined as the smallest value of acceleration required to activate a (ductile) plastic mechanism in the soil-retaining structure system. Potential plastic mechanisms must be correctly identified and depend on the layout of the retaining structure under examination.

Gravity and semi-gravity cantilevered walls accumulate permanent displacements either by sliding on their base or by bearing capacity failure. Ultimately, the type of plastic mechanism effectively mobilised within the soil-wall system depends on the strength of the backfill and of the foundation soil. The available evidence, including results of physical and numerical modelling and theoretical analyses, indicates that bearing capacity failure eventually leading to both sliding and rotation of the wall is likely to be the natural failure mechanism for walls resting on cohesionless foundation soils, whereas a mechanism of pure sliding controls the dynamic behaviour of the wall in undrained conditions. In either case, once the critical acceleration is attained, *i.e.*, as soon as a plastic mechanism develops in the soil-wall system, the absolute acceleration of the system remains approximately constant, even for increasing free-field acceleration.

The structural design of semi-gravity cantilevered walls must account for the soil thrust effectively acting on the stem of the wall, resulting from the dynamic interaction

between the soil volume above the heel and the wall. Up to the critical condition, Mononobe-Okabe pseudo-static solution provides a good estimate of the active soil thrust acting on the vertical stem. As soon as a plastic mechanism develops within the soil-wall system, the average absolute acceleration of the system remains constant at the critical value. However, the maximum shear force and bending moment in the stem of the wall can still increase due to an internal redistribution of stresses leading to a reduction of the shear stresses at the contact between the heel and the soil above it. A pseudo-static solution for the soil thrust acting on the vertical stem obtained neglecting any shear stress at the contact between the heel and the soil above it and using the critical seismic coefficient defines an upper bound for both the maximum shear force and the maximum bending moment in the stem of the wall.

A modified version of Newmark's method in which the wall-soil wedge system is assimilated to an elementary system comprising two-rigid blocks sliding on an inclined plane can be used to compute the permanent displacements of gravity and semi-gravity walls sliding on a rigid base. Further work is required to develop simple and reliable methods to predict the permanent displacements for walls where the critical mechanism corresponds to the attainment of bearing capacity of the foundation, as direct application of the Newmark's sliding block procedure can lead to significant under-prediction of the final displacement when the plastic mechanism comprises both translation and rotation of the wall.

Several factors make the seismic design of yielding embedded retaining structures more complex than that of gravity and semi-gravity walls. Full mobilisation of soil passive strength below dredge level, required to guarantee the stability of the wall, requires finite permanent displacements of the wall making the assumption of rigid perfectly plastic behaviour not conservative. Moreover, the definition of the critical plastic mechanism is not trivial given that no simple equivalent sliding block can be identified and the collapse mechanism is often characterises by diffuse plastic deformation. In particular, for anchored steel sheet pile walls, it is possible to identify at least three failure mechanisms involving full mobilization of the shear strength in the soil. Two of these are local failure mechanisms, corresponding to the attainment of anchor capacity or to the full mobilisation of the strength of the soil below dredge level, respectively. The third one corresponds to the activation of a global mechanism, involving the wall, the anchor plate and the soil volume interacting with them.

For embedded walls, the calculation of maximum shear forces and bending moments is always required for their structural design, preferably by simple limit equilibrium methods for the evaluation of both the pseudo-static contact earth-pressure distributions and the critical acceleration. Based on a clear understanding of the physical mechanisms governing the dynamic behaviour of these systems, pseudostatic limit equilibrium solutions have been illustrated for the analysis of both embedded cantilevered and anchored walls overcoming limitations of standard approaches available in the literature. Both for cantilevered walls and for anchored walls experiencing local failures the maximum internal forces are basically independent of the earthquake intensity and turn out to be a property of the system, with a tendency for the maximum internal forces to

increase with the strength, and hence the critical acceleration, of the system. For anchored walls experiencing global failure, the bending moment in the wall and the anchor forces may increase above the values computed for the critical acceleration.

The important issue of the calculation of permanent displacements of embedded walls has been dealt with only marginally in the paper. However, it is essential to recognise that, contrary to what happens for gravity and semi-gravity walls, significant displacements occur before the strength of the system is fully mobilised. Direct application of Newmark's like procedures, based on the rigid perfectly-plastic soil assumption, would yield displacements that are much smaller than observed, as the analysis would overlook the displacements experienced by the wall before the acceleration reaches its critical value.

References

1. Al Atik, L., Sitar, N.: Seismic earth pressures on cantilever retaining structures. J. Geotech. Geoenv. Eng., 136(10), 1324-1333 (2010).
2. American Association of State Highway and Transportation Officials. AASHTO.: LRFD Bridge Design Specifications. 6th Ed. Washington DC (2012).
3. Anderson, D.G., Martin, G.R., Lam, I., Wang, J.N.: Seismic analysis and design of retaining walls, buried structures, slopes, and embankments. NCHRP Rep. 611, Transportation Research Board, Washington, D.C (2009).
4. Callisto, L.: On the seismic design of displacing earth retaining systems. Proc. 7th International Conference on Earthquake Geotechnical Engineering, Rome, Italy (2019).
5. Callisto, L., Del Brocco, I.: Intrinsic seismic protection of cantilevered and anchored retaining structures. Proc. SECED Conf. on Earthquake Risk and Engineering Towards a Resilient World. Cambridge, UK (2015).
6. Caputo, G., Conti, R., Viggiani, G.M.B., Prüm, C.: Theoretical framework for the seismic design of anchored steel sheet pile walls. Proc. 7th Int. Conf. on Earthquake Geotechnical Engineering, Roma, Italy (2019).
7. Caputo, G., Conti, R., Viggiani, G.M.B., Prüm, C.: Improved Method for the Seismic Design of Anchored Steel Sheet Pile Walls. J. Geotech. Geoenvir. Eng., 147(2) (2019).
8. Cattoni, E., Salciarini, D., Tamagnini, C.: A Generalized Newmark Method for the assessment of permanent displacements of flexible retaining structures under seismic loading conditions. Soil Dyn. Earthquake Eng., 117, 221-223 (2019).
9. Conti, R.: Numerical modelling of centrifuge dynamic tests on embedded cantilevered retaining walls. Italian Geotech. Journal, 51(2), 31-46 (2017)
10. Conti, R., Madabhushi, S.P.G., Viggiani, G.M.B.: On the behaviour of flexible retaining walls under seismic actions. Géotechnique, 62(12), 1081-1094 (2012).
11. Conti, R., Viggiani, G.M.B.: A new limit equilibrium method for the pseudostatic design of embedded cantilevered retaining walls. Soil Dyn. Earthquake Eng., 50, 143-150 (2013).
12. Conti, R., Viggiani, G.M.B., Cavallo, S.: A two-rigid block model for sliding gravity retaining walls. Soil Dyn. Earthquake Eng., 55, 33-43 (2013).
13. Conti, R., Viggiani, G.M.B, Burali d'Arezzo, F.: Some remarks on the seismic behaviour of embedded cantilevered retaining walls. Géotechnique, 64(1), 40-50 (2014).
14. Conti, R., Madabhushi, G.S.P., Mastronardi, V., Viggiani, G.M.B.: Centrifuge dynamic tests on gravity retaining walls: an insight into bearing vs sliding failure mechanisms. Proc. 6th

International Conference on Earthquake Geotechnical Engineering, Christchurch, New Zealand (2015).
15. Conti, R.: Simplified formulas for the seismic bearing capacity of shallow strip foundations. Soil Dyn. Earthquake Eng., 104, 64-74 (2018).
16. Conti, R., Caputo, G.: A numerical and theoretical study on the seismic behaviour of yielding can-tilever walls. Géotechnique, 69(5), 377-390 (2019).
17. European Committee for Standardization. EN 1998-5:2004: E. Eurocode 8: Design of structures for earthquake resistance-Part 5: Foundations, retaining structures and geotechnical aspects. Brussels (2004).
18. Evangelista, A., Scotto di Santolo, A., Simonelli, A.L.: Evaluation of pseudostatic active earth pressure coefficient of cantilever retaining walls. Soil Dyn. Earthquake Eng., 30(11), 1119-1128 (2010).
19. Fusco, A., Viggiani, G.M.B., Madabhushi, G.S.P., Caputo, G., Conti, R., Prüm, C.: Physical modelling of anchored steel sheet pile walls under seismic actions. Proc. 7th Int. Conf. on Earthquake Geotechnical Engineering, Roma, Italy (2019).
20. Fusco, A.: Seismic behaviour of anchored steel sheet pile walls in sand. PhD Thesis. University of Cambridge, UK (2022).
21. Garini, E., Gazetas, G., Anastasopoulos, I.: Asymmetric 'Newmark' sliding caused by motions containing severe 'directivity' and 'fling' pulses. Géotechnique, 61(9), 733-756 (2011).
22. Huang, C.C.: Seismic displacement of soil retaining walls situated on slope. J. Geotech. Geoenvir. Eng., 131(9), 1108-1117 (2005).
23. Huang, C.C., Wu, S.H, Wu, H.J.: Seismic displacement criterion for soil retaining walls based on soil strength mobilization. J. Geotech. Geoenvir. Eng., 135(1), 74-83 (2009).
24. Itasca. FLAC Fast Lagrangian Analysis of Continua v. 5.0. User's Manual (2005).
25. Kloukinas, P., Mylonakis, G.: Rankine solution for seismic earth pressures on L-shaped retaining walls. 5ICEGE. Santiago Chile (2011).
26. Kloukinas, P., Scotto di Santolo, A., Penna, A., et al.: Investigation of seismic response of cantilever retaining walls: limit analysis vs shaking table testing. Soil Dyn. Earthquake Eng., 77: 432-445 (2015).
27. Koseki, J., Tatsuoka, F., Watanabe, K. et al.: Model tests of seismic stability of several types of soil retaining walls. In Reinforced Soil Engineering: Advances in Research and Practice (Ling HI, Leshchinsky D and Tatsuoka F (eds)), New York, NY, USA, 317-358 (2003).
28. Koseki, J., Koda, M., Matsuo, S., Takasaki, H., Fujiwara, T.: Damage to railway earth structures and foundations caused by the 2011 off the Pacific Coast of Tohoku Earthquake. Soils Found., 52(5), 872-889 (2012).
29. Lancellotta, R.: Lower-bound approach for seismic passive earth resistance. Géotechnique, 57(3), 319-321 (2007).
30. Ling, H.I.: Recent applications of sliding block theory to geotechnical design. Soil Dyn. Earthquake Eng., 21(3), 189-197 (2001).
31. Mononobe, N., Matsuo, H.: On the determination of earth pressure during earthquake. Proc. 2nd World Engineering Conference, Vol. 9, 177-185 (1929).
32. Mylonakis, G., Kloukinas, P., Papantonopoulos, C.: An alternative to the Mononobe-Okabe equations for seismic earth pressures. Soil Dyn. Earthquake Eng., 27(10), 957-969 (2007).
33. Newmark, N.M.: Effects of earthquakes on dams and embankments. Géotechnique, 15(2), 139-160 (1965).
34. NTC.: Aggiornamento delle Norme Tecniche per le Costruzioni. Rome, Italy: Ministero delle Infrastrutture e dei Trasporti (2018).

35. Oliynyk, K., Conti, R., Viggiani, G.M.B., Tamagnini, C.: A Generalized Newmark Method with displacement hardening for the prediction of seismically–induced permanent deformations of diaphragm walls. Submitted to Géotechnique (2022).
36. Okabe, S.: General theory of earth pressure and seismic stability of retaining wall and dam. Journal of Japanese Society of Civil Engineering, 12(1) (1924).
37. Pender, M.J.: Foundation design for gravity retaining walls under earthquake. Proceedings of the Institution of Civil Engineers - Geotechnical Engineering, 172(1), 42-54 (2019).
38. Pender, M.J., Conti, R., Caputo, G., Viggiani, G.M.B.: Discussion: Foundation design for gravity retaining walls under earthquake. Proceedings of the Institution of Civil Engineers – Geotechnical Engineering, https://doi.org/10.1680/jgeen.18.00125 (2019)
39. PIANC (Permanent International Association of Navigation Congresses): Seismic Design Guidelines for Port Structures. Balkema, Rotterdam, Netherlands (2000).
40. Richards, R., Elms, D.G.: Seismic behaviour of gravity retaining walls. J. Geotech. Eng. Div., ASCE, 105(4), 449-464 (1979).
41. Smith, C.C., Cubrinovski, M.: Pseudo-static limit analysis by discontinuity layout optimisation: application of seismic analysis of retaining walls. Soil Dyn. Earthquake Eng., 31(10), 1311-1323 (2011).
42. Stamatopoulos, C.A., Velgaki, E.G., Modaressi, A., Lopez-Caballero, F.: Seismic displacement of gravity walls by a two-body model. Bulletin of Earthq. Eng., 4, 295-318 (2006).
43. Verdugo, R., et al.: Seismic performance of earth structures during the February 2010 Maule, Chile, earthquake: Dams, levees, tailings dams, and retaining walls. Earthquake Spectra, 28(S1), S75-S96 (2012).
44. Viggiani, G.M.B., Conti, R.: On the behaviour of gravity retaining structures under seismic actions. Proc. 1st Int. Conf. on Natural Hazards and Infrastructure, Chania, Greece (2016).
45. Wagner, N., Sitar, N.: On seismic response of stiff and flexible retaining structures. Soil Dyn. Earthquake Eng., 91, 284-293 (2016).
46. Whitman, R.V., Liao, S.: Seismic design of retaining walls. Miscellaneous Paper GL-85-1, U.S. Army Engineer Waterways Experiment Station, Vicksburg, Mississippi (1985).
47. Zeng, X., Steedman, R.S.: Rotating block method for seismic displacement of gravity walls. J. Geotech. Geoenv. Eng., 126(8), 709-717 (2000).